Anbar Journal of Engineering Science (AJES) **Vol. 14 , No. 1 (2023) , pp. 15 ~ 30**
P-ISSN: 1997-9428 ; E-ISSN: 2706-7440 DOI: http://doi.org/10.37649/aengs.2023.137730.1035

University of Anbar

Anbar Journal of Engineering Science©

journal homepage: https://ajes.uoanbar.edu.iq/

Study of Some Durability Properties of Self-compacting Concrete Containing Waste Polyethylene Terephthalate

Marwah Majid Hameed[a], Mahmoud Khashaa Mohammed[b]

[a, b] *Department of Civil Engineering/ University of Anbar / Iraq*

PAPER INFO

Paper history:
Received 09/01/2023
Revised 16/02/2023
Accepted 28/02/2023

Keywords:
SCC , PET
Durability
Saline environment
Sulphate
ASR
Chloride.

ABSTRACT

This study investigates the durability properties and microstructural changes of self-compacting concrete (SCC) incorporating waste polyethylene terephthalate (PET) as fibers and fine aggregate replacement. This is after exposure to a saline environment (Alkalies, Sulphates, and Chlorides). PET effect into two forms was also evaluated for routine rheological properties of SCC and mechanical strength before and after exposure to sulphate salt. Five proportions of each form of PET incorporation in SCC mixtures were utilized. The volume fractions considered for PET as fibers were (0.25, 0.5, 0.75, 1.0, and 1.25)% by volume, with an aspect ratio of 28%, and (2, 4, 6, 8, and 10)% by volume for fine aggregate replacements. Results indicated that the inclusion of PET adversely affected fresh propertis especially high proportions of PET as fine aggregate. Alkali silica reaction (ASR) outcomes illustrated an enhancement in the PET fibers mix, while fine-PET mix was slightly enhanced. Magnesium sulphate reduced mass and compressive strength of all mixes in percentages ranging from (0.18-0.90) % for mass loss and (0.47-55.13) % for compressive strength loss. Ultrasonic pulse velocity (UPV) and dynamic modulus of elasticity (Ed) increased due to the sulphate impact except for M0.5 and M10, which decreased in both tests. Chloride's theoretical and modelled results illustrated higher diffusion coefficients and lower surface chloride content of fiber-PET mixes than fine-PET mixes. The predicted SCC cover depths for fiber-PET mixes were lower than those predicted for fine-PET mixes for 20 and 50 years of service life design.

1. Introduction

The most often utilized building material in the construction sector is concrete. Compaction is necessary after casting conventional concrete to provide adequate strength and durability. Improperly compacted concrete will have voids, resulting in poor-quality concrete. In addition, inadequate compaction increases concrete's permeability, which is a function of the durability of concrete structures [1]. Due to the high permeability of concrete cover, aggressive agents, especially carbon dioxide and chlorides can penetrate reinforced concrete causing frequent durability issues such as steel reinforcement corrosion[2]. Therefore, new types of concrete should be invented to overcome this common problem. Self-compacting concrete (SCC), a special kind of High-Performance Concrete HPC, has changed the possibilities available to the building sector regarding durability. It needs no compaction

* Corresponding authors: Marwah Majid Hameed, E-mail: mar20e1020@uoanbar.edu.iq

as compared to traditional concrete. SCC can consume high amounts of waste as a partial replacement for cement. Wastes, on the other hand, are a significant environmental issue and could harm the ecosystem [3].

Reusing and discarding these wastes are crucial. Recycling and reusing wastes are two methods that the construction industry may consider [3][4]. Plastic is the most often used man-made material worldwide due to its unique properties, ease of manufacturing and molding, low cost, and low density. Its limited biodegradability and existence in huge amounts led to a deleterious environmental influence [5]. One of the most used plastics is polyethylene terephthalate (PET). It is used in water and soft drinks bottles and many other things. That means huge amounts of plastic are discarded on land [6]. Numerous attempts have been made to evaluate the performance of plastic in concrete to reduce this waste and the cost of concrete structures. Recycled plastic has been applied in two ways: fibers to strengthen brittle concrete and enhance some of their mechanical characteristics, or as a partial or complete substitute for aggregates [6]. In the current work, PET is utilized as both fibers and as a partial replacement of fine aggregate in a sustainable SCC.

It is common knowledge that climate change can affect natural systems, altering rainfall patterns, melting ice caps, rising sea levels, and other phenomena. It is anticipated that, in the following decades, the consequences of climate change will become increasingly significant everywhere globally. The effects of greenhouse gas emissions being postponed in time, regardless of warming forecasts and the degree of mitigation policy effectiveness. Global environmental and social situations would become unstable as a result of any change in the climate. These perturbations may threaten the preservation of natural ecosystems and the sustainability of socioeconomic systems. Climate change's economic, environmental, and social effects must thus be considered in many different study domains, including structural engineering [7][8]. There are few studies concerning the effect of including plastic waste and studying its impact on concrete related/exposed to perturbations resulting from climate change which is mostly related to the durability properties of concrete. It is also related to the construction sector in the rise of salts and chemical materials due to industrial expansion and global warming [7]. Thus, in this study, experiments were done to investigate the impact of plastic waste on concrete exposed to aggressive environments with different types of chemicals/ salts such as alkalies, sulfates, and chlorides. The effect of incorporating PET in SCC is also evaluated regarding routine fresh tests of SCC.

Plastic wastes (PET) were used in two types in this investigation, producing advantages, first, decreasing abandoned PET by getting rid of them and providing landfills, second, conserving natural resources. This investigation's possible positive/negative results would be considered a significant solution that can be improved/enhanced to face the future effects of climate change and plastic industrial expansion side effects or disadvantages.

Giaccio et. al. [9] examined the fiber-reinforced normal concrete for its residual properties after ASR. They studied the generated cracks, expansion, and mechanical properties for prisms and cylinders cast and tested at ages (28 and 370) days using three types of fibers (steel, macro polymer and micro polymer). The results revealed that incorporating fibers enhanced the concrete's resistance to ASR. This is by reducing the quantity and width of the cracks, even in high alkalinity solutions where the fiber-containing concrete showed better results than plain concrete. Also, the impact of ASR on blocks of fibers reinforced concrete left outdoors and exposed to climate changes was studied by Giaccio et al. [10]. Their concrete prisms were left in the laboratory at 20°c and monitored for expansion, crack patterns, and air permeability for three years using different types of aggregate (reactive and nonreactive). The results indicated- despite not inhibiting ASR- they reduced deformation and cracks. The variance of results was lower in concretes containing fibers, where the decrement in expansion after incorporating steel and polymer fibers after two years was about (35 and 25) %, respectively, when compared to plain concrete. Bhogayata and Arora [11] reinforced concrete with post-consumed metalizes plastic (MPW) obtained from the disposed food packaging plastics, shredding them into macro fiber with lengths of (5, 10, and 20) mm mixing them with concrete in a range of (0-2) % fraction by volume. The researchers then tested concrete for durability issues such as sulphate attack, chloride penetration, acid attack, and corrosion. The results indicated a reduction in the

mass of the samples and a reduction in compressive strength. This could be due to the expansion of ettringite resulting from sulphate attack, which generated inside pressure in concrete.

Further, due to the formation of newly components throughout the cement hydrated matrix leading to disruptive actions to occur. Raman and Jaiganesan [12] used nondestructive tests such as Shmedit Rebound hammer and Ultrasonic Pulse Velocity (UPV) to evaluate the effect of adding plastic (polystyrene) as fine aggregate replacement on the durability of SCC exposed to sulphate solution, the volume fractions were (10, 20, 30, 40, and 50) % of fine aggregate. The results indicated a reduction in compressive strength for all percentages of replacement after sulphate attack. There was a loss in weight recorded and it was lower with the mixes containing plastic. The concrete showed a reduction in UPV values for all mixes after sulphate attack. Preethiwini [13] immersed cubic concrete specimens after the 28-days curing, for 60 days in a 5 % sodium sulphate solution. The concrete had plastic scrub obtained from disposed plastic materials as a substitution of fine aggregate with (0, 5, 10, 15, and 20) % by the weight of fine aggregate. The results illustrated no loss occurs in samples' mass; however, the compressive strength of all mixes showed a decrement by almost the same percentage for weight loss. Vijaya et. al. [14] involved nine percent of waste plastic fibers in self-compacting concrete to assess their resistivity against chloride penetration. The samples were immersed in a 5 % magnesium chloride solution for (30,60, and 90) days. The results indicated an enhancement of chloride resistance with increased plastic fiber content. Faraj et. al. [15] produced ten mixtures of self compacting high-strength concrete (SCHSC) with the incorporation of waste plastic particles as a fine aggregate replacement in addition to various percentages of mineral additions. This is to evaluate the mechanical and durability characteristics including sorptivity and chloride resistivity. The results illustrated an increment in sorptivity coefficient and chloride penetration with the increase in plastic content with no regard of the effect of curing time. Most of previous work on the effect of PET plastic on concrete considered their impact on the fresh and hardened properties in particular for SCC. However, very limited or no work has been done to examine the durability properties of SCC containing PET in terms of ASR, sulfate attack and chloride penetration in a qualitative and quantitative manners which is the main aim of the current research. The change in the microstructural properties due to the sulfate attack in PET – SCC (as fibers or fine aggregate) has not been studied yet and should be clarified clearly. The designing of concrete cover and service life prediction of PET – SCC in harsh environments of chloride has not been found in the literature. Thus, a durability design and modeling work have been done in this research for this purpose.

2. Limitations of the Study

The durability properties of the produced SCC in this research have been investigated and evaluated using accelerating regems. These properties include: alkali-silica reaction impact, sulphate attack and chloride penetration. This is due to time limitation for performing the long-term test. However, further studies should be implemented to cover this aspect.

3. Experemental Work

3.1 Materials

Sulphate resisting cement Type V was used as a binder material in all mixes. The cement meets the limits of Iraqi specification No. 5/2019 [16]. Tables 1 and 2 illustrate the cement's chemical and physical characteristics. The fly-ash used in this study is of type c, known as high calcium fly-ash, with chemical composition and physical properties as illustrated in Table 3. Natural fine sand available locally in Anbar Governorate was used after washing, cleaning, and drying it to eliminate scums, chloride impurities and sediment content. Characterstics of aggregate are shown in Table 4 compared to Ieaqi Specification No.45, 1984 [17] and ASTM C128 [18]. Equal weight quantities of crushed gravel with a maximum particle size of 10 mm from the Al-Nebai region were used as coarse aggregate in all concrete mixtures. A high range water reducing and super-plasticizing additive of Sika ViscoCrete-5930 L were used. Recycled PET (RPET) in this study obtained from discarded soft drink bottles shown in Figure 1 was used in two forms (fibers addition with dimensions of 3mm width, 30 mm length, and aspect ratio (l/d) of 28 and fine aggregate replacement passing through 4.75mm sieve) with the earlier proportions.

Table 1 Chemical Composition of Sulphate Resisting Cement

Compound	Oxide	Oxide % by Weight	Limit of I.Q.S No.5/2019 [16]
Ca	CaO	65.35	-
Si	SiO_2	20.21	-
Al	Al_2O_3	4.39	-
Fe	Fe_2O_3	5.71	-
Mg	MgO	2.53	≤ 5.0
S	SO_3	2.28	-
Main Compound			
Element Oxide %	C_3S 68.2	C_2S 6.5	C_3A 1.98 / C_4AF 17.4

Table 2 Physical Characteristics of Sulphate Resisting Cement

Characteristic	Test Result	Limit of I.Q.S No.5/2019 [16]
Specific gravity (g/cm^3)	3.16	-
Specific surface area (m^2/kg)	325	≥ 280
Initial setting time (minutes)	165	≥ 45
Final setting time (hours)	3.55	≤10

Table 3 Chemical Composition of Fly-ash

Compo-und	CaO	SiO_2	Al_2O_3	Fe_2O_3	MgO	SO_3	K_2O
% by Weight of Fly-ash	27.4	30.2	6.4	27.66	0.27	0.9	2.7
Physical Characteristics	Density (g/cm^3)			0.571			
	Specific gravity			2.58			

Table 4 Properties of Natural Aggregate (Fine and Coarse)

Property		Sulphate Content SO3	Specific Gravity (SSD)	Fineness Modulus	Water Absorption %
Result	Fine	0.1	2.64	3.3	0.81
	Coarse	0.05	2.62	5.9	0.53
Limit of Specification		≤ 0.5 for fine ≤ 0.1 for coars	-	-	-
Specification		I.Q.S No.45/1984 [17]	ASTM C128 [18]	I.Q.S No.45/1984 [17]	ASTM C128 [18]

(a) **(b)**

Figure1 Waste PET
(a)PET fibers (b) PET fine aggregate passing through 4.75mm

3.2 Mix Design

The first step of experimental work was designing a reference mix (RM) with several attempts to have a mix that satisfies the EFNARC specification [19][20]. The other mixes were designed in two ways, one by adding PET fibers as an addition to the RM with five proportions (0.25, 0.5, 0.75, 1.0, and 1.25), and the other way by replacing fine aggregate with fine PET with also five proportions (2, 0.5% fiber addition and 6% fine replacement are named as M0.5 and M6 respectively. Table 5 illustrates PET mix design and proportions in the SCC mixes. The water-to-binder ratio w/b was kept constant at 0.286 and adopted for all mixes. The SP was 1.05% of the binder weight. 4, 6, 8, and 10). The mixes were given names according to the PET content used. For instance, the 0.5% fiber addition and 6% fine replacement are M0.5 and M6, respectively. Table 5 illustrates PET mix design and proportions in the SCC mixes. The water-to-binder ratio w/b was kept constant at 0.286 and adopted for all mixes, and the SP was 1.05% of binder weight.

3.3 Testing

3.3.1 Fresh Properties Tests

Immediately after mixing, the concrete is tested for flow ability (by slump flow and T_{500mm} tests), passing ability (using L-box test), and the segregation index SI (by sieve segregation test) according to the EFNARC guideline [19]. This investigates the impact of adding PET to SCC in two used forms (fibers and fine aggregate). Table 6 shows the limits for fresh properties represented

by EFNARC guideline [19]. Figure 2 shows images of fresh properties tests.

Table 5 Mix Design and Proportions of PET

Mix name	Cement (kg/m³)	Coarse Agg. (kg/m³)	Sand (kg/m³)	Fly-Ash (kg/m³)	Water (kg/m³)	SP (kg/m³)
RM	400	765	860	170	165	6
Mix name	With fibers					
Constituent (kg/m³)	M0.25	M0.5	M0.75	M1	M1.25	
Cement	400	400	400	400	400	
Coarse Agg.	765	765	765	765	765	
Sand	860	860	860	860	860	
Fly-Ash	170	170	170	170	170	
Water	165	165	165	165	165	
SP	6	6	6	6	6	
PET	3.4	6.9	10.3	13.8	17.2	
Mix name	With fine aggregate					
Constituent (kg/m³)	M2	M4	M6	M8	M10	
Cement	400	400	400	400	400	
Coarse Agg.	765	765	765	765	765	
Sand	851	842	833	824	815	
Fly-Ash	170	170	170	170	170	
Water	165	165	165	165	165	
SP	6	6	6	6	6	
PET	9	18	27	36	45	

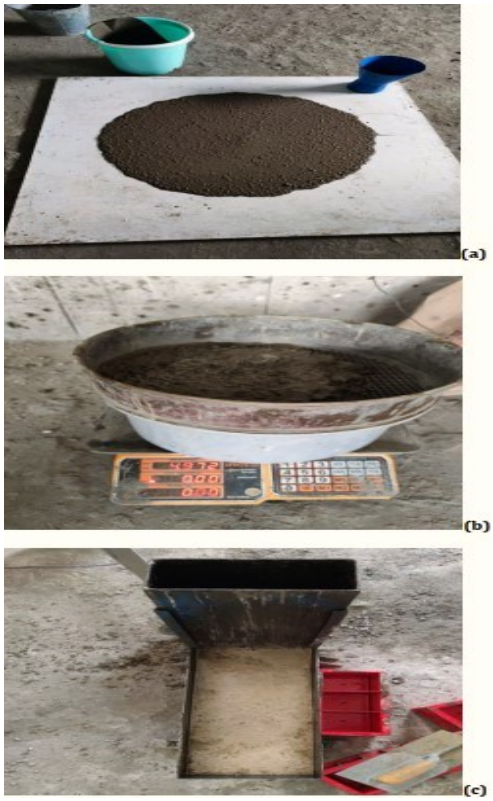

Figure2 Fresh properties tests (a) Slump flow (b) Segregation resistance (c) Blocking ratio

Table 6 EFNARC Limits for Fresh SCC [19]

Test Name	Class	Value
Slump flow(mm)	SF1	550-650
	SF2	660-750
	SF3	760-850
T_{500mm} time (sec)	VS1	≤ 2
	VS2	2-5
L-box blocking ratio (H_2/H_1)	PA1	≥ 0.8 with two bars
	PA2	≥ 0.8 with three bars
Segregation Index	SR1	≤ 20
	SR2	≤15

3.3.2 Hardened Durability Properties

I. Alkali Silica Reactivity Test (ASR)

This test method, shown in Figure 3 identifies whether an aggregate used in concrete could experience an ASR that might lead to internal expansion. ASTM C1260 [21] was utilized for this purpose. The reference mix RM and one proportion of each form of PET (fibers and fine aggregate) were tested in this test. Two different sample shapes were used. Considering the PET size, samples with dimensions of (28.5 × 7 × 7) cm were used for 0.75% fiber addition.

In contrast, samples with dimensions of (16 × 4 × 4) cm were used for 6% fine aggregate replacement. The test procedure may be summarized as follows: after 24 h of casting and being covered with nylon sheets, the specimens were placed in containers ending 16 days of exposure to 80°C heat and immersed in water. Then, they were set in an oven at 80°C for another 24 h, and a zero reading was recorded at the end of the duration using a digital caliper with 0.002 mm accuracy.

Figure 3 ASR Test

The specimens were placed into containers having 1M NaOH solution via full immersion inside an oven at 80°C for 14 days. The records of specimens' length had been taken at 4, 7, 11, and 14 days. ASTM C1260 [21] revealed that if concrete expansion was less than 0.1% after 16 days from casting indicates harmless activity.

II. Impact of Sulphate Environment on PET-SCC

This test aims to investigate the impact of sulfate environment on the properties of SCC containing PET. No specific test or standard details the sulfate impact, but it can be conducted from the change in some of its characteristics such as: weight, compressive strength, and UPV. This is in addition to the change in microstructure tested by Scanning Electron Microscopy (SEM) and Energy-Dispersive X-ray (EDX). This study tested these properties on 12 cubic samples of 100mm in dimension for each form mix after 28 days of water curing. This is through wetting and drying cycles every 7 days in a solution of 20% Magnesium Sulfate ($MgSO_4$) for 56 days. The weight was recorded at 7 days intervals while compressive strength, SEM, and EDX were tested (before and after 56 days of exposure). UPV is also tested at the same ages as SEM and EDX. Figure 4 shows the details and test of SCC exposed to sulphate salt.

Figure 4 Sulfate Impact on SCC Test

III. Scanning Electron Microscopy (SEM) and Energy-Dispersive X-ray (EDX)

Scanning electron microscopy (SEM) uses a targeted electron beam on an element's surface to study its microstructure. In SEM, the electrons interact with atoms in the sample at various depths, producing various signals that contain information about the surface topography and composition of the sample conducted as pictures. While EDX can be used to identify the chemical elements in a sample and evaluate their relative abundance by making a hole in the inner shell of an atom. This is by detecting the x-ray with higher energy reflecting from the sample's surface. The following criteria as described in many investigations [22] were used to evaluate the EDX test:

C-S-H $[0.8 \le Ca/Si \le 2.5, (Al+Fe)/Ca \le 0.2]$

CH $[Ca/Si \ge 10, (Al+Fe)/Ca \le 0.04 \text{ and } S/Ca \le 0.04]$

AFm $[Ca/Si \ge 4.0, (Al+Fe)/Ca > 0.4 \text{ and } S/Ca > 0.15]$

IV. Chloride Penetration Test

Using 100mm concrete cubes, the chloride penetration test was conducted according to the guidance of the NT Build 443 standard [23]. After casting, demolding, and curing for 28 days in water, the samples were fully submerged in a sodium chloride solution with a 2M concentration (165 gm/L) for 90 days. The cubes were then sealed from five faces in two layers of paint to ensure that only one direction of chloride penetration would occur perpendicular to the casting director. After 90 days, the specimens were taken out of the solution and let to dry. Powder of 3-4 grams samples was collected from each cube using a drill to make holes in the cube at different distances (1, 5, 7, 11, and 15) mm. The chloride contents were determined at Al-Ain Laboratory for Engineering Tests. Chloride test process is shown in Figure 5.

Figure 5 Chloride Penetration Test Process.

The surface chloride concentrations (C_s) and apparent chloride diffusion coefficients (D_{nss}) were computed from the concentration and depth relationship. With the help of the Excel solver tool, the curve fitting was based on a numerical solution utilizing the least squares method for reducing

errors between the obtained experimental findings and the theoretical model. The data's theoretical model depends on the best solution of Fick's second low (Eq 1), as mentioned in NT BUILD 443 [23].

$$C(x,t) = C_s - (C_s - C_i) \cdot erf\left(\frac{x}{\sqrt{4D_{nss} \cdot t}}\right) \ldots\ldots \quad (1)$$

Where:
C(x,t) = chloride content measured at depth x at exposure time t, % by weight of concrete.
C_s = calculated surface chloride content, % by weight of concrete.
C_i = initial chloride content, % by weight of concrete.
x = depth (mm)
D_{nss} = apparent chloride diffusion coefficient (non-steady state), m^2/sec
t = exposure time (sec)
erf = error function= erf (z)= $\frac{2}{\sqrt{\Pi}} \int_0^z exp(-u^2)\, du$

To estimate long-term diffusion, the most well-known governing mechanism for the chloride ingress process (submerged concrete structure), the short-term values (D_{nss} at 90 days) must be changed to a time-dependent value as expressed in Eq 2.

$$D_a(t) = D_{ao}(t)\left(\frac{t_o}{t}\right)^{\alpha} \ldots\ldots\ldots\ldots \quad (2)$$

Where:
$D_a(t)$=Time dependent chloride diffusion coefficient.
t: Maturity age and to: Reference maturity age (when concrete is exposed to chloride).
D_{ao}: Obtained apparent chloride diffusion coefficient (D_{nss}) at (t_o).
α: Aging factor (reduction in Dnss with time due to continuous hydration plus binding effect, taken as 0.6 for FA SCC) [22].
For various exposure humidity and circumstances, the essential chloride content for steel corrosion initiation is between 0.05-0.07 by weight of concrete and is typically accepted as 0.05% by weight of concrete [22]. As shown in Figures later in the discussion of results, the intersection of horizontal line (Cl concentration of 0.05% by weight of concrete) with the vertical line indicates the predicted depth of concrete cover required for the structure at 20 and 50 years.

4. Results and discussion

4.1 Fresh Properties Outcomes

The performance of fresh mixes had been determined to assess the effect of adding PET on the deformability, stability, and consistency of SCC. Four basic properties were tested: filling-ability, viscosity, resistance to segregation, and passing ability.

A. Slump Flow

Figure 6 shows the results of slump flow of all 11 tesed mixtures in this study. The range of slump flow dimeters for fiber PET-SCC were from 747.5mm for M0.25 to 875mm for M1.25. The results showed that the lower incorporations of PET fibers were better in filling ability than the higher incorporation percentages. The M0.75 and M0.25 values were higher compared to RM. This behavior could be referred to as the distribution of fibers in the mix and the phenomena of fibers balling, which causes aggregate and other mix's fine materials to be trapped and unable to move freely in some mixes. That was most noticed in the M1.0 and M1.25 as the fiber content increased.
As for fine PET replacement, there was a notable decrease in flow diameters for all mixes. However, the flow in SCC containing 4% sand replacement increased slightly more than RM. There was variance in results with incorporation of PET where the lowest percent of fine PET showed a decrement in value more than the other percentages. The 10% showed a lower value than 2%. That can be referred to the large amounts of PET particles which need more paste to wrap it and might be due to the increase of inner fraction between PET particles and other constituents.

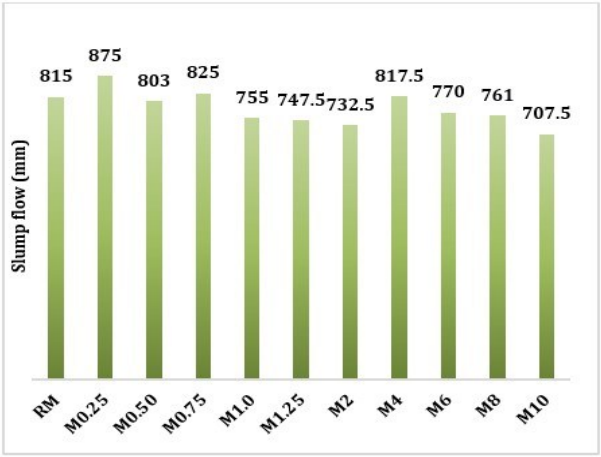

Figure 6 Slump Flow Diameters for SCC Mixtures

B. Flow Time T_{500mm}

$T_{500mm,}$ SI, and L-box results are illustrated in Figure 7. There was an increase in T_{500} values which is an inverse trend compared to flow diameters. They increased with the increments of PET content in the two incorporation forms. That indicates a rise in the viscosity of mixes, making them need longer to reach the required flow. Also, it was noticed that the mixes having PET as fibers had a lower flow time than the mixes with PET fine aggregate. This could be due to the large surface area of PET fibers compared to PET particles which allow the mix to flow. It had also been seen that the flow time of SCC mixtures containing PET fibers was lower than those containing PET as fine particles. According to EFNARC guidelines for T_{500}, the produced SCC mixtures can be categorized as VS2 except for the RM, which is VS1. The (8 and 10) % of fine PET incorporations are out of the SCC limits for T_{500mm}.

C. Segregation Index SI

Sieve segregation test was used to assess the stability of mixes and the reliability of segregating or bleed. Figure 7 revealed that the inclusion of PET slightly inversely affected the resistance to segregation in all mixes using the two types of PET incorporations. However, they were still within the limits of EFNARC. M1.0 and M1.25 were exceptions where their SI was out of EFNARC limits. The M2 of fine PET substitution showed the best behavior regarding segregation resistance with a value of 9.8%. It is thought that the inclusion of PET fibers/particles produced excessive water, which can increase mix segregation.

D. Blocking Ratio

The ratio H2/H1 representing the height variance between the two ends of the L-box mold, should be between 0.8 and 1 to produce a well-passing ability. As shown in Figure 7, mixes containing PET fiber were more affected by the increment in PET content. The M1 and M1.25 showed a full blockage through the reinforcing bars. This behavior might be due to the large quantity of fibers which acted like a wall blocking the aggregate behind it and finally prohibiting the paste from coming through the bars. The lower content of PET expressed an enhancement in H2/H1 and the smooth surface of the fibers thought to be worked as an assistant to minimize friction within paste movement. The mixes with PET as fine aggregate enhanced the mixes' passing ability, especially with the lower proportions of the fine PET. However, the higher proportions showed a decrement in H2/H1. The full blockage did not occur as in the mixes with fiber-PET showing that the use of waste plastic as fine aggregate was better than as fibers in this aspect. It is thought that the increase in fine-PET particles having angular ends with inner friction increment led to obstructing concrete movement through reinforcing bars.

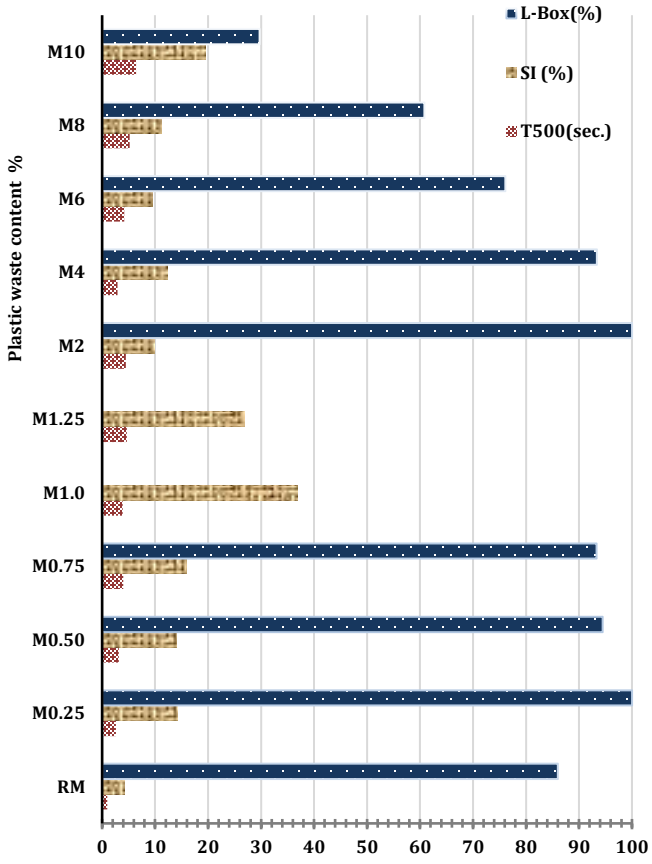

Figure 7 Fresh Properties of SCC Mixtures

The variance in fresh properties' results also had been noticed in the research results. Most of them confirmed the adverse effect of including PET in SCC, especially on the flowability and passing ability such as Al- Hdithi and Hilal and Jakowska et. al. [6][24]. While K.Aswatama [25] illustrated an improvement in all the fresh properties of PET-SCC. However, Mohammed [26] noticed an enhancement only in the flow diameters. However,

there was a decrement in L-box ratio and segregation resistance in the study.

4.2 Durability Properties

I. Alkali Silica Reactivity (ASR)

As mentioned in section 3.3.1, one percentage of each form of PET mix (0.75% fiber addition and 6% fine aggregate replacement) was tested and compared with RM. The expansion of each sample (i.e., change in length) and the expansion ratio were calculated and drawn in Figure 8. The results showed an enhancement of the ASR resistance with adding fibers. The expansion ratio for M0.75 was 0.02% which is lower than RM1's value (0.1%) and within ASTM C1260 [21] limits. This indicates an increase in the bonding of paste constituents and hence, restriction of concrete expansion due to fibers leading to better resistance against alkali reactivity.

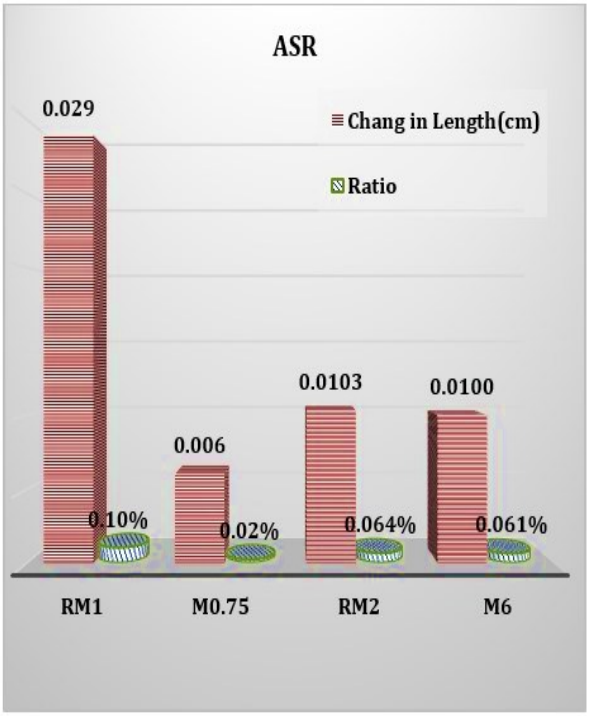

Figure 8 Expansion Amounts and Ratios due to ASR

As for the M6 fine aggregate replacement, there was a slight decrease noticed in SCC expansion. RM2 expanded by (0.0103cm) while M6 of (0.01cm). The expansion ratio was (0.064%) for RM2 and (0.061%) for M6. This indicates that the fine PET presents a low/no bonding that could enhance the resistance to alkali reactivity. However, the ratio of both mixes (i.e., RM2 and M6) is considered to be neglected as they are less than the limit explained by the standard as mentioned earlier (0.1%). Giaccio et al. [9][10] also showed an enhancement in concrete's expansion and width of cracks in normal concrete containing steel and polymer fibers.

II. Sulphate Resistance Results

It can be determined through some changes noted on the samples as described in the following points:

A. Visual Observation

The SCC specimens' dimensions remained unchanged. Nevertheless, efflorescence was seen on the surface of the immersed specimens as shown in Figure 9, as time progresses and the cycles of drying and immersing increase.

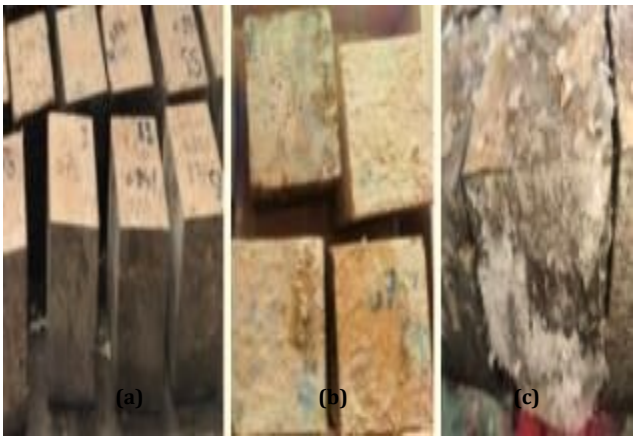

Figure 9 Crystallization of Sulphate Salts on Samples (a) Before Immersion (b), (c) After Progress of Time- Dry and wet Specimens, Respectively

B. Mass Loss

The immersion of samples in 20% magnesium sulphate solution for 56 days in cycles of wetting and drying each 7 days led to a change in the mass of the mixes for the two forms of PET (as fibers and as fine aggregate), as shown in Table 7.

The results indicated losses in the mass of all mixes, including RM. However, some loss was lower than RM which can be considered an enhancement in sulphate resistance of mixes M0.5, M1.25, M6, M8, and M10. While other mixes, such as M0.75 ad M4 showed a higher value in loss percentage compared to RM with 0.9% and 0.83% respectively. In general, the mixes containing fine- PET showed

lower values for mass losses percentages as illustrated in Figure 10.

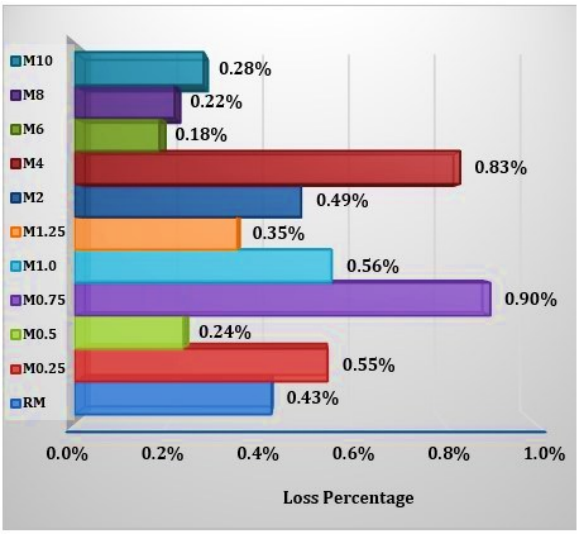

Figure 10 Percentage Loss of Mass after Immersion in Magnesium Sulphate for 56 Days

Their loss percentages were lower than mixes of fiber-PET, especially with the high substitute of PET. The cement paste volume in concrete or mortar often increases when exposed to sulfate. The expansion and deterioration of concrete can be attributed to the diffusion of sulfate ions from the soil, groundwater, and seawater into the hydrated cement paste and their reaction with C_3A in the presence of $Ca(OH)_2$ to create ettringite and gypsum [27].

The deterioration mechanism due to magnesium sulphate attack might be due to forming ettringite, gypsum, and brucite $Mg(OH)_2$, which retards the negative effects of sulphate at an early age. However, in the later stages, the decomposition of C-S-H gel and its transformation to M-S-H gel occur, leading to softening in the binder and reduction in mechanical strength [28].

C. UPV Results after Sulphate Attack

The UPV of the samples were taken before and after immersion in 20% magnesium sulphate at (0 and 56) days respectively. The results in Table 8 indicated an increase in the values of UPV of all mixes except for the M0.5 which decreased slightly. The formation of ettringite and gypsum in addition to brucite $Mg(OH)_2$ and salts crystallization inside concrete might led to fill the voids in concrete and finally retarding the time of waves to reach the other face of the sample.

Table 7 Mass Change Results due to Sulphate Salt

Mixes	0-Day	14-Day	28-Day	56-Day	Loss percentage
RM	2403	2393	2398	2393	0.43%
M0.25	2437	2432	2435	2424	0.55%
M0.5	2411	2405	2389	2405	0.24%
M0.75	2412	2411	2400	2390	0.90%
M1.0	2398	2385	2387	2385	0.56%
M1.25	2404	2399	2396	2396	0.35%
M2	2382	2386	2381	2370	0.49%
M4	2387	2384	2369	2367	0.83%
M6	2366	2358	2351	2361	0.18%
M8	2363	2355	2359	2358	0.22%
M10	2311	2321	2327	2305	0.28%

Table 8 UPV Values before and after Sulphate Attack

RM		0- Day		56- Day	
		4.22		4.49	
Fiber-PET Mixes					
Mixes\ Days	M0.25	M0.5	M0.75	M1.0	M1.25
0	4.18	4.21	4.02	4.16	3.93
56	4.47	3.94	4.21	4.38	4.32
Fine-PET Mixes					
Mixes\ Days	M2	M4	M6	M8	M10
0	4.2	4.11	4.06	3.92	4.32
56	4.55	4.43	4.41	4	4.04

E. Change in Dynamic Modulus of Elasticity (E_d)

Due to the alteration in UPV and density values after exposure to sulphate salt, E_d changed its values for all mixes. Figure 11 shows the change percentage for E_d and UPV values before and after immersion in magnesium sulphate for all mixes. The results illustrated an increase in E_d for the two forms of PET inclusion and RM. However, the M0.5 and M10 expressed a decrement in their values. This behavior is more related to the change in UPV than the change in density where the latter expressed decrement in value for all SCC. The same factors affected the increase in UPV are affecting E_d.

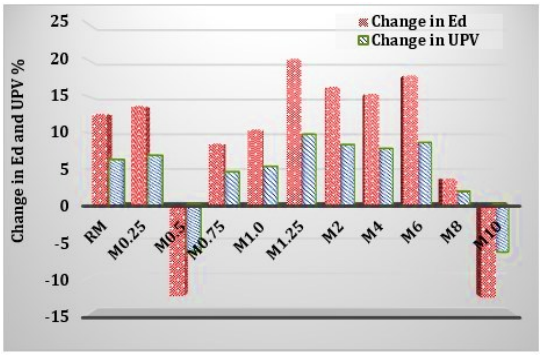

Figure 11 Change Percentage in E_d and UPV due to Sulphate Salt between Initial and Final Values

F. compressive Strength Reduction Outcomes

The compressive strength results of the mixes were recorded at four periods of exposure time (0, 14, 28, and 56) days. The loss percentage in compressive of RM was 18.7%. These percentages of fiber-PET and fine-PET mixes are shown in Figure 12. M1.0 and M10 gave the higher loss percentages than RM with (19.4 and 55.1) % respectively. It was noticed that at the first 28 days, there was an increase in compressive strength values. However, the compressive strength decreased with the increase of time and at the end of the test. The increase in values might be referred to the formation of brucite $Mg(OH)_2$, which retards the negative effect of sulphate attack as mentioned previously. Also, the transformation of C-S-H gel to M-S-H gel led to weakening the binder and finally reducing the compressive strength.

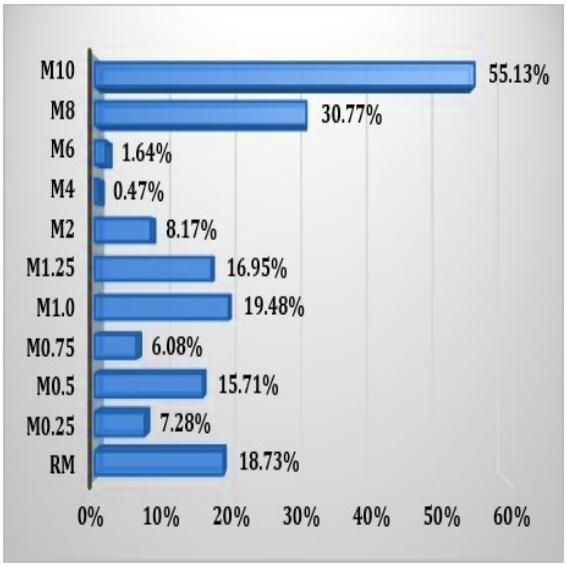

Figure 12 Percentage Loss of Compressive Strength after Immersion in Magnesium Sulphate for 56 Days

G.Microstructure Tests Outcomes

The samples used for this test were the M1.0 fiber addition and M8 fine aggregate replacement compared to RM results. Based on the criteria mentioned previously for determining the presence of C-S-H (Calcium Silica Hydrates) gel, CH (Ca(OH)2), and AFM (Ettringite) in section 3.3.2 III, samples were tested before and after (at 56 days) immersion in MgSO4. The results of hydration products are illustrated in Table 9.

Depending on the criteria above, the analysis depended on the variance in Ca/Si and S/Ca ratios for determining the changes in hydration products. The CSH gel, CH, and AFM for RM at the beginning of the test were detected according to the limits of the criteria. However, the increase in Ca/Si value over the upper limit after 56 days of sulphate exposure means that the gel was decomposed and transformed into ettringite, which was limited to equal or more than 4.0. The ratio of S/Ca confirmed the lack of AFM before exposure to sulphate and assured its presence after 56 days of sulphate immersion. In addition to AFM, the C/Si confirms the formation of $Ca(OH)_2$ (i.e. CH).

Table 9 Presence of C-S-H, CH, and AFM in RM, M1.0 and M8

Hydration Products	Criteria	Results					
		RM		M1.0		M8	
		Day 0	Day 56	Day 0	Day 56	Day 0	Day 56
C-S-H	0.8 ≤ Ca/Si ≤ 2.5	1.78	4.2	/*	2.93	/*	7.21
CH	Ca/Si ≥ 10 S/Ca ≤ 0.04	1.78	4.2	/*	2.93	/*	7.21
		0.06	0.006	/*	0.023	/*	0.006
AFM	Ca/Si ≥ 4 S/Ca > 0.15	1.78	4.2	/*	2.93	/*	7.21
		0.06	0.006	/*	0.023	/*	0.006

It is thought the CSH could react with the $MgSO_4$ leading to the formation of brucite $Mg(OH)_2$. This expanded compound and extra ettringite with larger crystals and secondary hydration products generate an inside pressure on the concrete and

produce additional microcracks. These cracks allow more solution into the concrete, reducing its strength. Figures 13, 14, and 15 show some mixes' SEM images before and after exposure to sulphate attack, confirming the EDX analysis presented in Table 9.

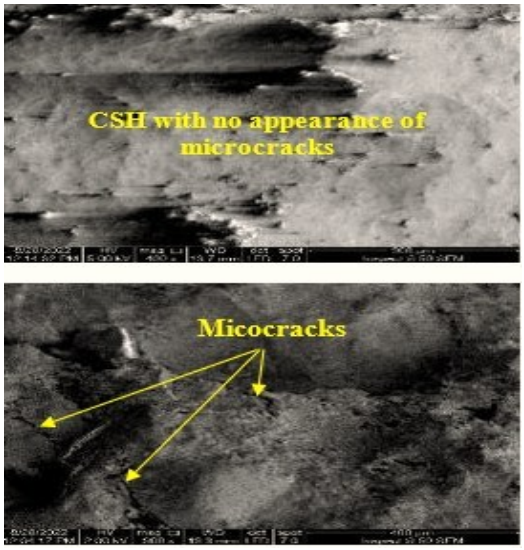

Figure 13 SEM Images for RM microstructure Before and After Exposure to Magnesium Sulphate Respectively

Figure 14 SEM Images for M8 microstructure Before and After Exposure to Magnesium Sulphate Respectively

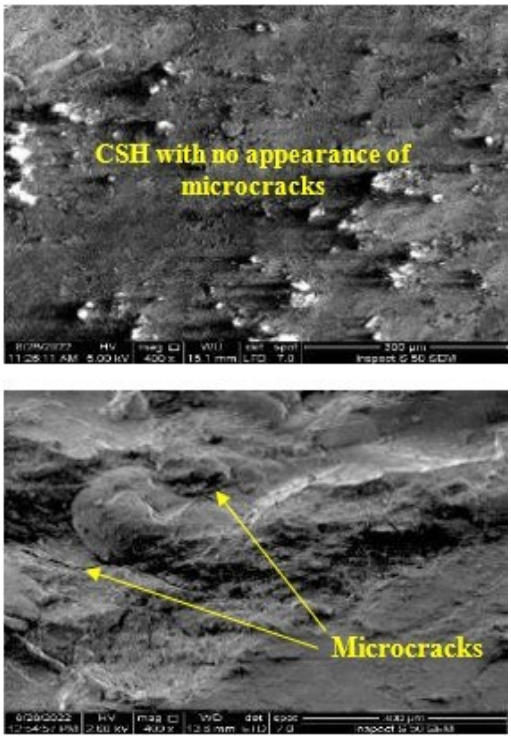

Figure 15 SEM Images for M1.0 microstructure Before and After Exposure to Magnesium Sulphate Respectively

For the M1.0 mix analysis, a slight increase in Ca/Si ratio was found before exposure. The little presence of AFM after exposure as detected by EDX analysis might mean that the CSH gel did not fully decomposed. This decomposition did not lead to form large amount of ettringite. The S/Ca ratio of 0.023 means that there is a formation of AFM after 56 days but with a small amount compared to RM. This means that the pressure generated inside M1.0 mix was lower than RM indicating a benefit of using the plastic as fibers in SCC.

M8 mix showed a similar behavior of RM in term of ettringite formation after sulphate attack. The ratio of Ca/Si noticed to be increased above the limits of CSH gel and AFM after 56 days assuring the decomposition of CSH and its transform to AFM. This might be due to the reaction between $MgSO_4$ and hydration products with the presence of $Ca(OH)_2$ in accordance the value of S/Ca obtained after exposure to sulphate. This indicates that the use of plastic as fine aggregate did not enhance the sulphate resistance of SCC. In general, M1.0 showed a better performance than RM and M8.

H. Chloride Penetration Results

The chloride penetration test was used to evaluate the apparent diffusion coefficient (D_{nss}) and surface chloride concentration (C_s) for SCC. They were obtained from the best fitting of the relationship between chloride concentrations (% by weight of concrete) and the penetration depth (mm). Least square method was used to reduce the square sum of errors between the experimental results obtained in laboratory and the theoretical model with the utility of excel solver tool. Figure 16 shows the curve best fitting of RM. Depending on Nordtest method NT BUILD 443 [23], the best solution of Fick's second low of diffusion (Eq 1) was used to plot the theoretical model in RM's figure and other mixes. The points before maximum point detected when their chloride contents lower than the maximum are cancelled from the non-linear regression curve. Due to the leaching of chloride to the sample's surface; these points usually appear in the relationship between depth and chloride content [22]. The values of D_{nss} and C_s are listed in Table 10 for SCC mixes.

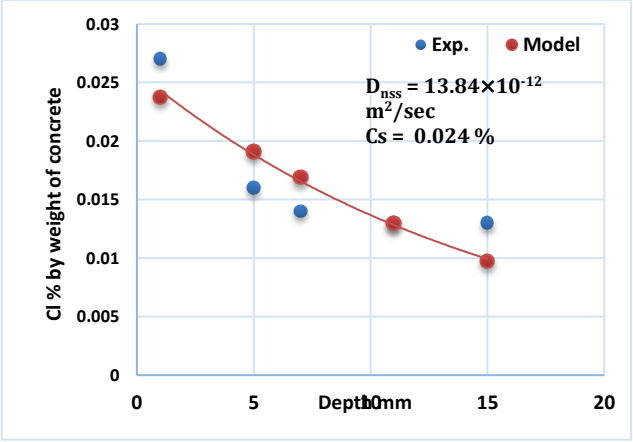

Figure 16. Using Excel Solver for Curve Fitting Data for RM

RM had a diffusion coefficient of 13.84×10^{-12} m^2/sec which is higher than some mixes, although it had a lower surface content of chloride (0.024%) compared to other PET-mixes. However, the modelling of RM's results illustrated that (7and 9) mm might be used as minimum covers for a durable service life design for 20 and 50 years, respectively. This is for concrete structures exposed to 0.02% chloride content by weight of concrete.

Table 10 D_{nss} and C_s values for SCC

Mix	D_{nss} $\times10^{-12}$ (m^2/sec)	C_s (%by weight of concrete)
RM	13.84	0.024
M0.25	8.5	0.15
M0.5	16.2	0.133
M0.75	7.54	0.091
M1.0	9.3	0.083
M1.25	21.8	0.086
M2	47.59	1.36
M4	29.94	1.43
M6	7.66	2.49
M8	3.21	4.07

The results for fiber- PET mixes illustrate a close values of apparent diffusion coefficient (7.54-9.3) $\times10^{-12}$ m^2/sec for the M0.25, M0.75, and M1.0. However, M0.5 and M1.25 showed higher diffusion coefficient values than other mixes. This might refer to the increase of pores inside SCC due to the inclusion of PET fibers. However, the theoretical cover design of these types of concrete (as shown in Table 11) indicated cover values of only 25mm and 30mm to ensure service lives of 20 and 50 years for M0.5 respectively.

Results regarding C_s illustrated that M0.25 has the highest content of surface chloride in comparison with other mixes, although, it has a low apparent diffusion coefficient (higher chloride resistance) compared to M0.5 and M1.25. On the other hand, M1.25 had low surface chloride concentration despite having the lowest chloride resistance (high chloride diffusion coefficient D_{nss}).

As for fine-PET mixes, the apparent diffusion coefficient values were decreasing with the increase in fine-PET replacement. The possible reason for this behavior might be that the PET fine particles increased the path of chloride penetration at higher ratios. Th lowest chloride diffusion coefficients were 3.21×10^{-12} m^2/sec and 7.54×10^{-12} m^2/sec foR M8 and M0.75 mixes respectively. This indicates that the use of plastic as a fine aggregate is better to reduce the chloride diffusion coefficients. However, higher surface chloride concentration detected in these mixes leads to need higher cover to protect the steel from corrosion as shown later on in this section (Table 11).

Using D_{nss} and C_s obtained from Excel solver tool based on the best solution of Fick's second law as illustrated in Eq1 helps to estimate the service life numerically to find C(x,t) for various ages. Chloride movement's interacted mechanisms through concrete are hydration and diffusion. Thus, the

short-term obtained values (Dnss at 90 days expressed in Table 10) have to be modified to a time-dependent value to predict the long-term diffusion coefficient [22]. Eq2 is used for long-term prediction for chloride penetration considering the D_{nss} obtained earlier and the aging factor (α), which had been taken as 0.6 for FA based concrete.

The steel corrosion initiates with chloride content ranging from (0.05-0.07) % by weight of concrete for various humidity and conditions of exposure. These values had been considered as the critical chloride content and normally taken as 0.05% by weight of concrete [22]. The intersection between 0.05% (the horizontal line) with the modelling curve at any age leads to predict the depth of concrete cover required to resist chloride ingress till that age, as shown in Figure 17 for M1.0. The concrete cover designed theoretically for M1.0 should be (11 and 13) mm minimum to fulfill (20 and 50) years of service life respectively. Based on results obtained for predicted cover, the fiber-PET mixes produced cover depths lower than those presented by fine-PET mixes.

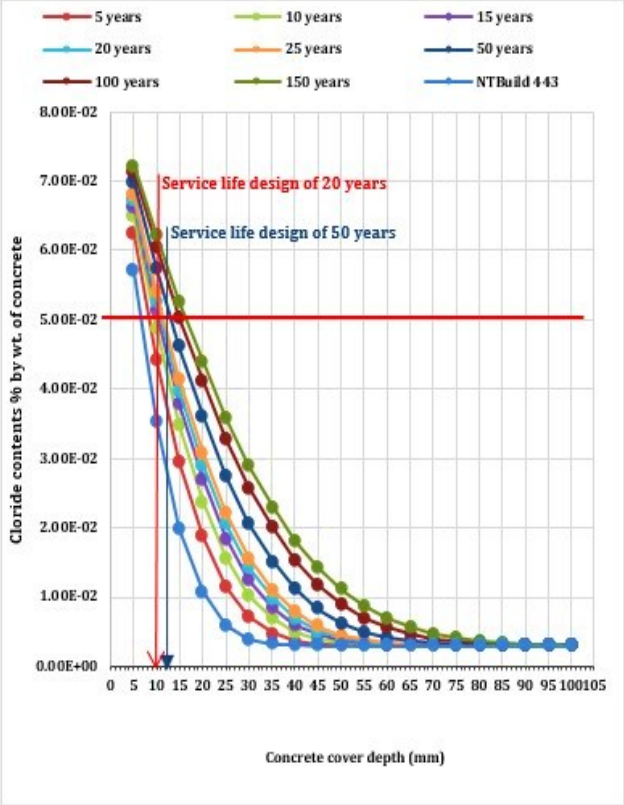

Figure 17 Chloride Penetration Model for M1.0

Table 11 Theoretical Designed Covers for SCC

Mix Name	Theoretical 30Designed Covers (mm)	
	20 years	50 years
M0.25	19	24
M0.5	25	
M0.75	12	14
M1.0	11	13
M1.25	18	22
M2	93	112
M4	76	91
M6	41	51
M8	29	36

5. Conclusion

This study aims to investigate the impact of involving PET in SCC on the fresh and durability properties using two forms of PET (as fibers and as fine aggregate replacement). The following conclusions can be drawn: The involvement of PET in SCC (as fibers and fine aggregate replacement) adversely affected the fresh properties. M0.75 showed an enhancement in the resistance to ASR with a ratio of 0.02% compared to RM, indicating the role of fibers bonding with the paste which restricted the increase in length caused by ASR.

The effect of sulphate salt on SCC was observed through several aspects after 56 days of exposure to 20% MgSO4 solution as follows: Although the efflorescence on the surfaces of SCC samples by visual observation, there was no change in their dimensions. However, reductions in the mass loss were noticed in all mixes, including RM, with 0.43%. The increase in UPV values after exposure to sulphate salts had been noticed, except for the M0.5 which decreased slightly. Further, E_d values showed changes as well. Compressive strength showed reductions for all mixes. RM showed a 18% loss while the highest loss was for M10 (55%). EDX analysis illustrated a decomposition of CSH and the formation of CH and ettringite. SEM images confirm the conclusions derived from the EDX analysis.

Apparent chloride diffusion coefficients' (D_{nss}) values of fiber-PET mixes were close to RM's (13.48 $\times 10^{-12}$ m^2/sec). D_{nss} of fine-PET mixes decreased with the increase of PET content. In contrast, Cs were higher for all mixes than RM (0.024%). The predicted covers for 20 and 50 years of service life design indicated that M0.5 and M8 were within limits determined by Eurocode2 for minimum

cover required for durability for the structures exposed to chloride from seawater.

6. Suggestions for future work

This study focused on the effect of incorporating PET in SCC and investigating the impact on the durability properties in addition to the rheological. However, additional work should be conducted as follows: Using other types of discarded plastics as fine/coarse aggregate in SCC, such as wasted boxes used for transporting groceries and studying the durability and transported properties of this type of concrete. The current study uses the same sets of prepared SCC mixes to investigate the durability properties of concrete exposed to high temperatures or direct fire. Studying the effect of ASR on the SCC containing PET as fibers and as fine aggregate for longer periods and investigating the formation of cracks quantitatively using advanced microstructural testing such as SEM and MIP.

References

[1] V. R. Sivakumar, O. R. Kavitha, G. Prince Arulraj, and V. G. Srisanthi, "An experimental study on combined effects of glass fiber and Metakaolin on the rheological, mechanical, and durability properties of self-compacting concrete," *Appl. Clay Sci.*, vol. 147, no. January, pp. 123–127, 2017, doi: 10.1016/j.clay.2017.07.015.

[2] S. Rasiah, "Properties of Flowing Concrete and Self-Compacting Concrete With High-Performance Superplasticier Properties of Flowing Concrete and Self-Compacting Concrete With High-Performance Superplasticier," no. September, pp. 17–20, 2015.

[3] R. Dachowski and P. Kostrzewa, "The Use of Waste Materials in the Construction Industry," *Procedia Eng.*, vol. 161, pp. 754–758, 2016, doi: 10.1016/j.proeng.2016.08.764.

[4] B. Franco, A. M. Domingues, N. D. A. Africano, R. M. Deus, R. Aparecida, and G. Battistelle, "Sustainability in the Civil Construction Sector Supported by," *Infrastructures*, vol. 7, no. 43, pp. 1–23, 2022.

[5] R. Sharma and P. P. Bansal, "Use of different forms of waste plastic in concrete - A review," *J. Clean. Prod.*, vol. 112, pp. 473–482, 2016, doi: 10.1016/j.jclepro.2015.08.042.

[6] A. I. Al-Hadithi and N. N. Hilal, "The possibility of enhancing some properties of self-compacting concrete by adding waste plastic fibers," *J. Build. Eng.*, vol. 8, pp. 20–28, 2016, doi: 10.1016/j.jobe.2016.06.011.

[7] P. Croce, P. Formichi, and F. Landi, "Climate change: Impacts on climatic actions and structural reliability," *Appl. Sci.*, vol. 9, no. 24, 2019, doi: 10.3390/app9245416.

[8] A. Colette, "Case studies on climate change and World Heritage ," UNESCO World Heritage Centre, 2007.

[9] G. Giaccio, M. E. Bossio, M. C. Torrijos, and R. Zerbino, "Contribution of fiber reinforcement in concrete affected by alkali-silica reaction," *Cem. Concr. Res.*, vol. 67, pp. 310–317, 2015, doi: 10.1016/j.cemconres.2014.10.016.

[10] G. Giaccio, M. C. Torrijos, C. Milanesi, and R. Zerbino, "Alkali–silica reaction in plain and fibre concretes in field conditions," *Mater. Struct. Constr.*, vol. 52, no. 2, pp. 1–15, 2019, doi: 10.1617/s11527-019-1332-2.

[11] A. C. Bhogayata and N. K. Arora, "Impact strength, permeability and chemical resistance of concrete reinforced with metalized plastic waste fibers," *Constr. Build. Mater.*, vol. 161, pp. 254–266, 2018, doi: 10.1016/j.conbuildmat.2017.11.135.

[12] J. V. Marshall Raman, "Mechanical Studies of Self Compacting Concrete Using Plastic Aggregate," *Int. J. Res. Appl. Sci. Eng. Technol.*, vol. V, no. II, pp. 226–233, 2017, doi: 10.22214/ijraset.2017.2036.

[13] B. Preethiwini, S. Bharaniraja, M. Aravindhan, B. B. Pradeep, and R. Jothiprasath, "Comparative study on durability characteristics of high strength self compacting concrete," *Int. J. Civ. Eng. Technol.*, vol. 8, no. 3, pp. 942–949, 2017.

[14] G. S. Vijaya, V. G. Ghorpade, and H. Sudarsana Rao, "The Behaviour of Self Compacting Concrete with Waste Plastic Fibers When Subjected to Chloride Attack.," *Mater. Today Proc.*, vol. 5, no. 1, pp. 1501–1508, 2018, doi: 10.1016/j.matpr.2017.11.239.

[15] R. H. Faraj, A. F. H. Sherwani, and A. Daraei, "Mechanical, fracture and durability properties of self-compacting high strength concrete containing recycled polypropylene plastic particles," *J. Build. Eng.*, vol. 25, p. 100808, 2019, doi:

10.1016/j.jobe.2019.100808.
[16] Properties of Portland Cement, Iraqi Specification No.5, 2019.
[17] Natural Sources for aggregate that is used in concrete and construction, Iraqi Specification No.45, Baghdad, 1984.
[18] Standard Test Method for Relative Density (Specific Gravity) and Absorption of Fine Aggregate, ASTM C128-15, 2015.
[19] The European Guidelines for Self Compacting Concrete Specification, Production and Use, EFNARC, 2002.
[20] The European Guidelines for Self Compacting Concrete Specification, Production and Use, EFNARC, 2005.
[21] Standard Test Method for Potential Alkali Reactivity of Aggregates (Mortar-Bar Method), ASTM C1260-07, 2007.
[22] M.K. Mohammed "Multi-scale Response of Sustainable Self- Compacting Concrete (SCC) to Carbonation and Chloride Penetration" Ph.D. dissertation, *Univ. of Nottingham* ," 2015.
[23] Concrete, hardened: accelerated chloride penetration, BUILD, Nord Test. 443, 1995.
[24] J. Jaskowska-Lemańska, M. Kucharska, J. Matuszak, P. Nowak, and W. Łukaszczyk, "Selected Properties of Self-Compacting Concrete with Recycled PET Aggregate," *Materials (Basel).*, vol. 15, no. 7, 2022, doi: 10.3390/ma15072566.
[25] W. K. Aswatama, H. Suyoso, N. U. Meyfa, and P. Tedy, "The Effect of Adding PET (Polyethylen Terephthalate) Plastic Waste on SCC (Self-Compacting Concrete) to Fresh Concrete Behavior and Mechanical Characteristics," *J. Phys. Conf. Ser.*, vol. 953, no. 1, 2018, doi: 10.1088/1742-6596/953/1/012023.
[26] M. H. Mohammed "Production of SCC Using Local Waste Materials: Statistical Approach," *MSC thesis, Univ. Anbar, Coll. Eng.*, 2019.
[27] D. Bondar, C. J. Lynsdale, N. B. Milestone, and N. Hassani, "Sulfate Resistance of Alkali Activated Pozzolans," *Int. J. Concr. Struct. Mater.*, vol. 9, no. 2, pp. 145–158, 2015, doi: 10.1007/s40069-014-0093-0.
[28] H. Biricik, F. Aköz, F. Türker, and I. Berktay, "Resistance to magnesium sulfate and sodium sulfate attack of mortars containing wheat straw ash," *Cem. Concr. Res.*, vol. 30, no. 8, pp. 1189–1197, 2000, doi: 10.1016/S0008-8846(00)00314-8.